2014 IEEE International Conference on Robotics & Automation (ICRA)
Hong Kong Convention and Exhibition Center
May 31 - June 7, 2014. Hong Kong, China

Accurate In-Plane and Out-of-Plane Ultrasound-based Tracking of The Discretely Actuated Steerable Cannula

Elif Ayvali and Jaydev P. Desai

Abstract— **Discretely actuated steerable cannula is a multi-degree-of-freedom hollow needle (cannula) that could potentially be used in needle-based procedures to deliver therapeutic and diagnostic tools to a target region through its hollow inner core. Needle-based procedures are commonly performed using intra-operative image guidance. 2D ultrasound is one of the most commonly used imaging modalities in clinics. It is portable, inexpensive and free of ionizing radiation. The success of the needle-based procedures depends on accurate detection of the needle. The accuracy of the out-of-plane detection, where the ultrasound transducer is placed at a right angle to the long-axis of the needle, depends on the ultrasound beam width. Finite width of the ultrasound beam and uniform cross-section of the needle introduce errors in tracking. The accuracy of in-plane tracking depends on the tracking algorithm used and the spatial resolution of the ultrasound transducer. This work presents a method to quantify the finite ultrasound beam width and the spatial accuracy of the transducer. An out-of-plane detection method was implemented to locate the tip of the discretely actuated steerable cannula. An in-plane tracking algorithm based on optical flow was also developed to obtain the shape of a planar cannula. The algorithms and the methods developed in this work are general and they can be extended to needles having straight, curved and arbitrary shapes.**

I. INTRODUCTION

Needle-based procedures require the guidance of the needle to a target region to deliver therapy or to remove tissue samples for diagnosis. Needle insertion is commonly performed using magnetic resonance imaging (MRI), computed tomography (CT), fluoroscopy or ultrasound guidance. The success of image-guided procedures highly depends on the ability to precisely locate the needle and the anatomical structures. During needle insertion, needle deflection occurs due to needle-tissue interaction which deviates the needle from its insertion direction. Due to poor needle placement, multiple insertion attempts at a single site are often made by the physician. Furthermore, some sites are inaccessible using straight-line trajectories due to the anatomical structures that need to be avoided. There are many challenges in achieving accurate targeting in needle-based procedures, and hence there is no single solution to overcome these challenges. Modeling needle-tissue interaction is an important step to understand needle deflection. Needle deflection and tissue deformation models were developed to estimate the needle motion during insertion [3]. Externally manipulating the tissue to push obstacles away from the insertion path [14] or guiding the tumor towards the line of insertion of the needle [10] are effective approaches to improve the targeting accuracy. Robot-assisted needle insertion combined with image guidance is promising to improve the accuracy of the percutaneous procedures. The initial alignment of the needle with the target can be achieved with robotic assistance [4]. However, most of the targeting errors occur due to needle deflection when the needle is inside the soft-tissue. Manipulating the needle at the base provides limited control over the needle trajectory after the insertion. In our previous work, a multi-degree-of-freedom hollow needle (cannula) was developed to account for the needle placement errors once the needle is inside the soft-tissue [1]. The cannula is composed of straight segments that are connected by shape memory alloy (SMA) actuators at discrete locations along its length. When the SMA actuators are heated using resistive heating, they transform into an arc thereby generating joint torques. To control the bending angle at each joint and hence the tip of the cannula, two control approaches have been explored. One approach is to measure the bending angle or the tip position directly from the imaging modality. The second approach is an indirect approach where the strain of the SMA actuators is controlled by controlling the temperature of the SMA actuator. The constitutive model of the SMA relates the stress, strain and the temperature of the SMA. This work is focused primarily on the detection of the cannula in ultrasound-images for ultrasound-guided steering of the cannula. We are interested in combining in-plane and out-of-plane tracking of the cannula in the ultrasound images.

A. Ultrasound Image-based Tracking

Ultrasound is one of the most widely used imaging methods in medicine. Real-time ultrasound-based imaging can easily be done at any probe position or orientation which makes it attractive for instrument guidance in interventional procedures. The main challenge with ultrasound guidance in needle-based procedures is the artifacts produced by the needle [8]. The artifacts result in missing boundaries, rendering various portions of the needle invisible. Needle visibility depends on the alignment of the needle with the ultrasound imaging plane. The needle tracking can be achieved in-plane and out-of-plane. When the needle long axis and the needle tip lie in the same plane with the ultrasound beam, the tracking can be done in-plane. When the long axis of the needle is perpendicular to the plane of the ultrasound beam, the tracking is out-of-plane and only needle cross-section is visible. The transducer and needle alignment can be achieved

This work was supported by the National Institutes of Health (NIH) grant R01EB008713.

Elif Ayvali is with the Department of Mechanical Engineering, University of Maryland, College Park, USA, 20742. eayvali@umd.edu

Jaydev P. Desai is with the Department of Mechanical Engineering, University of Maryland, College Park, USA, 20742. jaydev@umed.edu

by sliding, tilting or rotating the transducer. Sliding the transducer across the needle is the most commonly used movement for aligning the ultrasound beam and the needle tip. Rotation of the transducer is required when the needle goes out of plane. There are many challenges in ultrasound-based tracking. In the out-of-plane tracking, only the cross-section is visible. Therefore, the shaft of the needle tip can be mistaken for the needle tip. The ultrasound transducer is usually placed at an angle with respect to the needle insertion direction to visualize the needle tip [7], [5]. In this approach, the detected cross-section can be the needle shaft and the needle tip can be at a greater depth. The in-plane tracking makes guidance easier since the entire needle can be seen. The imaging width of the ultrasound probe and the needle dimensions are commonly in mm scale. This sometimes makes it hard to align the needle long axis with the ultrasound beam.

B. Needle Detection and Image Analysis

Image analysis is widely applied to ultrasound images to reduce noise and extract useful information about the needle position. Extraction of lines, edges and curves is a key step in image analysis. The goal in out-of-plane tracking is to accurately detect the position of the needle tip whereas in-plane tracking requires finding geometry specific features of the needle. For a rigid needle, the feature to be detected can be a line whereas detection of local or global curvature may be required for a curved needle. The Radon transform is a well-known tool for detecting parametrized shapes in an image [6]. Radon transform was previously used to determine parametrized shapes of a curved needle [11]. Hough transform is commonly used to determine line parameters such as slope and intersection points and can be used to find the brightest line in an image [7], [13].

Needle is usually the dominant line in the ultrasound image. However, there might be gaps or other line artifacts that belong to other structures. To reduce the noise and detect the tip of the needle, thresholding or morphological operations such as erosion and dilation are commonly applied to the region of interest [12], [15]. Coating the needles with an echogenic coating such as Echo-Coat® (Angiotech Inc.) improves needle visibility. There are commercially available needles such as EchoBlock®, EchoSti® (Havel's Inc.) that have enhanced visibility compared to generic needles. Wrapping passive markers around the needle tip is another way of enhancing the needle shape in the ultrasound images [13]. One way to measure the location of the needle tip is to use a magnetic tracker attached to the needle at the tip. The tracker provides the relative position of the tip with respect to the magnetic tracker's base coordinate system. There are commercial systems for ultrasound guided biopsy. Logiq E9 ultrasound platform (GE Healthcare Inc.) and SonixGPS (Ultrasonix Inc.) utilize a miniaturized electromagnetic sensor for needle tracking. One of the sensors is embedded in the tip of a biopsy needle and another one to an ultrasound probe. The needle trajectory is displayed in real-time during an entire procedure.

C. Overview

This work is focused on detection of the cannula in-plane and out-of plane using ultrasound images. There are two important considerations in ultrasound-based tracking that are often overlooked. First, the ultrasound beam is commonly assumed to be infinitely thin. When the ultrasound probe is perpendicular to the needle tip, the detected shape is the cross-section of the needle. Since the geometry is cylindrical, each cross-section gives a circle. Even though the tip is accurately detected by the imaging algorithm, the spatial accuracy is still limited by the ultrasound beam width. Secondly, the spatial accuracy of the in-plane tracking depends not only on the accuracy of the algorithm but also on the resolution of the ultrasound transducer itself. These issues are addressed in this work. The paper is organized as follows. In Section II, the discretely actuated steerable cannula and the experimental setup used for tracking are introduced. To verify the in-plane tracking algorithm, a kinematic model of the cannula is required. The kinematics is also introduced in this section. In Section III, we demonstrate a method to quantify the ultrasound beam width and spatial accuracy. To detect the tip of the cannula, Hough circle transform was implemented. The method presented in this section provides a way to quantify and account for the error due to finite ultrasound beam width. An in-plane detection algorithm based on optical flow was developed to obtain the shape of the cannula. Finally, in Section IV we make some concluding remarks.

II. MATERIALS AND METHODS

A. Discretely Actuated Steerable Cannula

The cannula is composed of three straight segments made of polycarbonate with an inner diameter of 1.651 mm and outer diameter of 3.175 mm. The length of each section from the base to the tip is 3.8 cm, 2.5 cm, and 2.1 cm, respectively. There are two slots along the length of each straight segment and two antagonistic SMA actuators are placed at each joint. The SMA actuators are 0.53 mm in diameter and they are annealed in an arc shape. In this work, all SMA actuators lie in a plane. Hence, the cannula moves in a plane perpendicular to the location of the SMA actuators. The joints are covered with non-conductive rubber sheath for heat isolation and electrical insulation of the SMA actuators inside soft-tissue. The schematic of the cannula is shown in Fig. 1. There are 3 degrees-of-freedom (DOF): One DOF at each joint and one insertion DOF. The configuration of the cannula in a plane can be described using Eq. 1.

$$\begin{aligned} x &= L_1 + u + L_2 cos\alpha_1 + L_3 cos\beta + r_1 sin\alpha_1 \\ &\quad + r_2(sin\alpha_2 cos\alpha_1 - sin\alpha_1(1 - cos\alpha_2)) \\ y &= L_2 sin\alpha_1 + L_3 sin\beta + r_1(1 - cos\alpha_1) \\ &\quad + r_2(sin\alpha_1 sin\alpha_2 + cos\alpha_1(1 - cos\alpha_2)) \\ \beta &= \alpha_1 + \alpha_2 \end{aligned} \tag{1}$$

The joint angles, α_1 and α_2, are shown in Fig. 1. L_1, L_2, L_3 are the lengths of the straight segments from base to

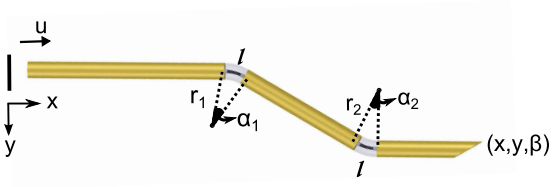

Fig. 1. Schematic used for kinematic model of a 3-DOF planar cannula

tip. The position of the tip is given by (x, y) and β is the orientation of the tip. The radius of curvature of the joints are given by r_1 and r_2. The relation between the arc radius, r, and joint angle, α, is $r = \ell/\alpha$ where ℓ is the length of the SMA actuator between consecutive links. The three equations representing the geometry of the cannula is solved using a 4^{th} order Runge-Kutta solver. The algorithm was implemented in C++.

B. Experimental Setup

The experimental setup used for ultrasound guidance is shown in Fig. 2. The frames are made of 1515 Lite framing material (80/20 Inc.). Two linear rail systems (Haydon Motion Solutions) were mounted to the frame, and they are used to control the ultrasound probe position in a plane. The rails consist of a stepper motor (size 17 double stack with 0.015875 mm per step resolution), a wedge style anti-backlash nut, an optical encoder (US Digital E5S, 500 counts per revolution), and 305 mm of total travel. The sliding element of the rails that move along the long axis of the rails have axial stability. However, it moves slightly when a loading is applied along its width. Rail 2 is mounted across the width of rail 1. To eliminate any horizontal movement that might occur during operation, rail 2 was also constrained using a guide rail that is attached on the frame. When rail 2 slides along the long axis of rail 1, it also slides along the guide rail that provides additional support. There is a DC motor (Model 247858, Maxon Precision Motors, Inc.) attached to the sliding element of rail 2, and its rotation axis is centered along the center of the ultrasound probe. Hence, the ultrasound probe has 3-DOF. The cannula is fixed between two plates that have a groove along their width. The plates are attached to a vertical support that is attached to the sliding element of rail 3. The height of the plates can be adjusted using screws. The vertical position of the ultrasound probe can also be adjusted prior to the experiments to make sure the ultrasound probe is in contact with the tissue sample. The arrows shown with dashed lines show the adjustment direction for the cannula fixture and the ultrasound fixture.

The ultrasound system is a Philips Sonos 5500 ultrasound console with a 3-11 MHz linear array transducer (Model 11-3L). Matrox Morphis (Matrox Inc.) frame grabber is used to grab frames in real time at 15 fps. The rails are controlled via a TTL-compatible motor control unit (DCM 8028, Haydon Motion Solutions) which directly drives the stepping motion of the motor. The TTL-signals are generated using Arduino UNO board at 500Hz and this frequency corresponds to 3.9 mm/s travel speed.

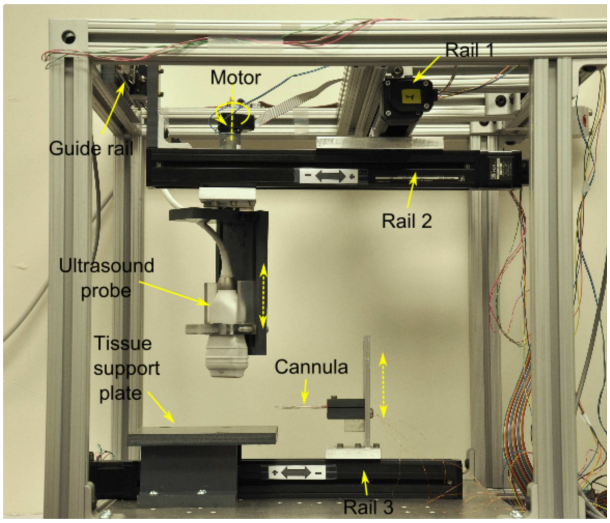

Fig. 2. Linear rail system used for ultrasound experiments

III. EXPERIMENTS AND RESULTS

This section presents the results of the out-of-plane tip detection and in-plane tracking of the cannula inside tissue phantom made of gelatin. For image analysis OpenCV library was used [2]. The algorithms were implemented in C++ on a Windows XP PC. In out-of-plane tracking, the transducer is positioned at right angles to the cannula insertion direction. The needle tip is found through image analysis as the transducer slides over the cannula. In in-plane tracking, the needle long axis is aligned with the ultrasound beam. Hence, the whole needle is visible. The needle tip position and orientation is obtained through image analysis. The corresponding bending angle at each joint can then be obtained using inverse kinematics.

A. Ultrasound Beam Width and Spatial Accuracy

To quantify the ultrasound beam-width, an object was scanned with the transducer and images were recorded with 0.127 mm increments. The physical dimension of the imaging window of the transducer is 4.7 cm x 1 cm. When the transducer is moved along the 'a' direction as shown in Fig. 3, the scanned object starts to appear after the dashed line. The object has maximum visibility when it is in the middle of the imaging window. The visibility decreases once the object passes beyond the center of the imaging window. The object and its dimensions are shown in Fig. 4a. Initially the transducer is away from the object and the object is not visible. The object starts to be seen at 0.381 cm, and the rectangular block disappears at 3.175cm. Fig. 4c shows the ultrasound images of the object at various locations. The rectangle block has 2.477 cm length and in the ultrasound images it is visible for 2.794 cm (3.175-0.381). That means the scanning width of the transducer is 0.317 cm (2.794-2.477). Even though the physical width of the probe is 1 cm, the effective imaging width is 0.317 cm. If an object with length L is scanned by sliding the transducer over the object,

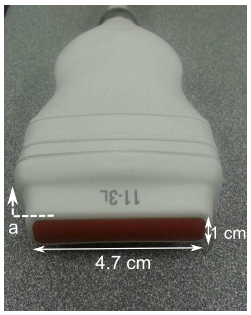

Fig. 3. 11-3L Linear Array Transducer

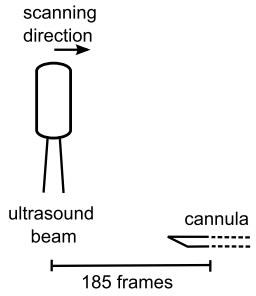

Fig. 5. The schematic of the experiment that was performed for out-of-plane detection of the cannula tip

the object will appear for $L + 0.317$ cm. If the transducer is used to track the tip of the cannula by placing the ultrasound probe orthogonal to the insertion direction, the tip is visible when the tip of the cannula is inside the 0.317 cm window. This means that the tracking accuracy of the tip is within 0.317 cm when the transducer is used to locate the tip of the cannula. The tip can be easily mistaken for the cannula shaft. This observation is important yet commonly neglected while assessing the accuracy of tracking the needle tip [12], [15].

To determine the image quality and spatial resolution of the transducer, the object shown in Fig.4a was scanned along its width. The dimensions of the cross-section is given in Fig. 4b. Fig. 4d shows several dimensions of the object measured using the cursor in the ultrasound console. The maximum error in dimensions was measured to be 0.015 cm. This implies that the spatial accuracy of in-plane tracking is limited by the spatial accuracy of the ultrasound.

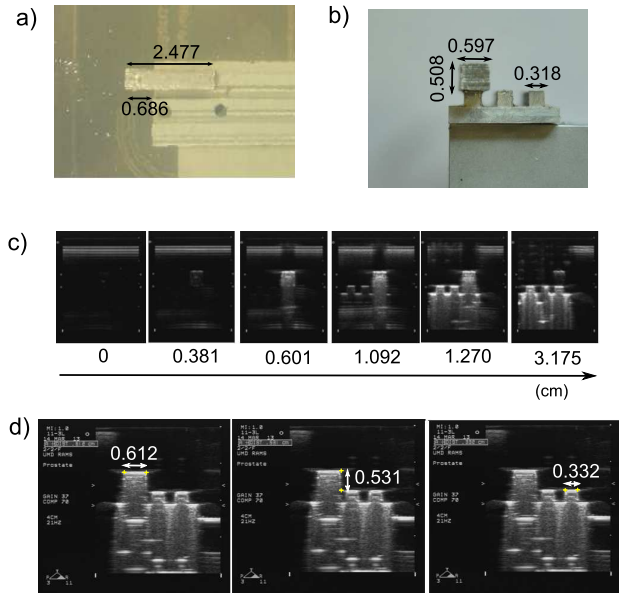

Fig. 4. Ultrasound beam width and spatial resolution experiments: a) The top view of the object that was scanned with the transducer, b) The front view of the object that was scanned, c) the ultrasound images of the object at different positions along the scanning axis, d) the dimensions of the object that were measured using the ultrasound console. The dimensions are in cm.

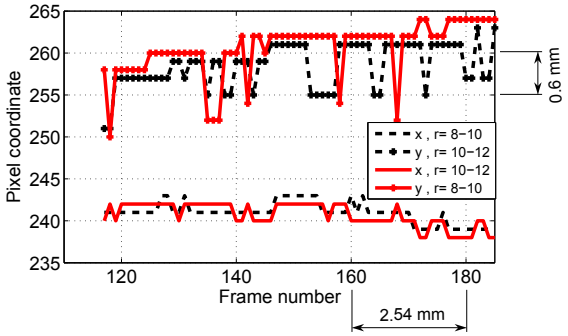

Fig. 6. The frames were recorded at 0.127 mm spacing. 20 frames correspond to 2.54 mm displacement of the transducer. 5 pixels correspond to 0.6 mm.

B. Out-of-plane Detection of the Cannula Tip

The ultrasound transducer is placed at right angles to the cannula as demonstrated in Fig. 5. The imaging depth was set to 8 cm. The initial position of the transducer is away from the cannula tip such that the cannula cannot be seen in ultrasound images. The transducer is moved towards the cannula tip with 0.127 mm increments and a total number of 185 ultrasound images were recorded. To detect the tip of the cannula, Hough circle transform was implemented. The ultrasound images were pre-processed using thresholding. Downscaling, upscaling, dilation, and erosion operations followed by blurring were applied recursively to obtain a clear image that is free of any noise. A range of pixel values can be specified to detect circles with a desired diameter. First the circle radius was specified as 8-10 pixel which corresponds to 3.074-3.842 mm diameter. A 10-12 pixel range was also tested for comparison since the cannula diameter can be larger in the ultrasound images due to artifacts. 10-12 pixel range corresponds to 3.842-4.610 mm diameter. Fig. 6 show the change in pixel coordinates of the detected circle as the transducer slides over the cannula tip. The result shows that both ranges give similar results and the first circle was detected at 117^{th} frame in both cases. Hence, 8-10 pixel range was used for detection of the tip. The ultrasound images and their corresponding frame number and position are given in Fig.7. The tip starts to appear at 75^{th} frame and the circle is detected after 42 frames (117-75). This corresponds to 5.334 mm displacement of the transducer. The

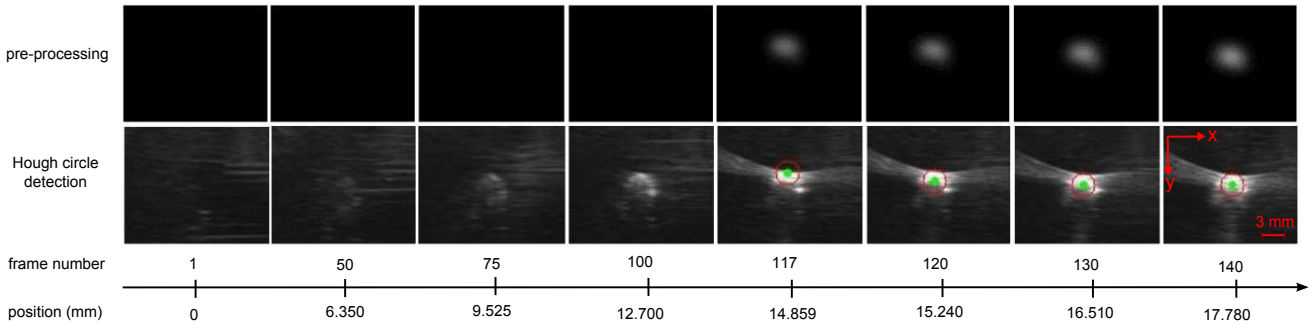

Fig. 7. The images at the top are obtained through pre-processing to reduce noise and enhance needle tip visibility. The images are then input into the Hough circle detection algorithm. The images at the bottom show the detected circles on the original ultrasound images.

length of the bevel-tip is 5.5 mm and the algorithm shows great performance in accurate detection of the tip. Based on the results of this study the following out-of-plane tracking method is proposed. As the cannula is inserted into soft tissue, the transducer will also move in the same direction. The transducer can be commanded to move the same distance as the insertion distance of the cannula. A better approach would be to displace the transducer based on the estimated position of the cannula tip. The transducer will also have a 6 mm sinusoidal motion (slightly larger than the bevel tip length) around the cannula tip to scan the bevel tip length. Therefore, the transducer will scan the whole bevel length while tracking the cannula to accurately detect the position of the tip. This approach accounts for the detection error due to finite ultrasound beam width and the uniform cross-section of the cannula.

C. In-plane Tracking of the Cannula

Lucas-Kanade optical flow is a powerful algorithm for motion detection. The algorithm uses sum-of-squared intensity differences as measurements to minimize the errors for each tracking and works with sub-pixel accuracy [9]. Optical flow algorithm is based on the brightness constancy assumption and hence it is sensitive to variation in brightness. Image brightness is not very stable in ultrasound images. The brightness of the whole image or certain regions (divided in rows) can be adjusted and speckle can be minimized by adjusting the settings on the ultrasound console. However, there is variation in brightness due to the artifacts caused by the cannula. Complete disappearance of tracked points due to sudden brightness change is rare but the tracked points can shift across pixels that have constant brightness. When the tracked points shift across the cross-section of the cannula due to pixels having similar brightness, it introduces an error in the angle calculation. To eliminate this problem, brightness variation of the tracked points in time should be minimized. To achieve this, the boundaries of the cannula can be enhanced using edge detection algorithms. An edge is defined by a discontinuity in gray-level values. Applying edge detection algorithms directly proves to be not useful since the artifacts of the cannula result in missing boundaries rendering various portions of the cannula invisible. Pre-processing of the images is necessary to reduce noise, brightness variation, and missing boundaries.

The image is first pre-processed using downsampling followed by upsampling operation to reduce the amount of noise and detail. Erosion, dilation and blurring operations are also applied recursively to reduce brightness variation and smoothen the image. The surface of the cannula facing the transducer has higher brightness in ultrasound images which makes edge detection useful. Sobel edge detection is applied to detect the top surface of the cannula. Finally, a linear blend operator is applied to the the final image obtained through Sobel edge detection and the original image. The blend operator overlays both images, thus enhancing the brightness of the top surface of the cannula on the original image.

For testing of the algorithm, a video of a cannula insertion experiment was recorded. The transducer was stationary and the cannula was inserted into the gelatin. The joint angles were varied randomly. The algorithm was tested on the videos to optimize the parameters of the tracking algorithm. Once the cannula is inside the imaging region, the tip of the cannula and one point on the top surface of the distal link are selected. A line is fitted between the two points and the bending angle of the first joint is obtained. The motion of the two points are continuously tracked using the pyramidal Lucas-Kanade optical flow algorithm. Fig. 8 shows the comparison of the optical flow algorithm implemented on the original image and the optical flow algorithm implemented after pre-processing and brightness enhancement. In the original optical flow algorithm with no brightness enhancement, the second point is shifted down across the needle cross-section. This shift results in error in the angle calculation. Fig. 9a shows the ultrasound images after pre-processing and edge-detection. A clean image is obtained and the upper surface of the cannula is detected. Fig. 9b shows the cannula and the kinematic model overlayed on the same image in real-time. The optical flow algorithm gives the pixel location of the cannula tip position and orientation.

The in-plane tracking method presented in this section can also be applied to rigid and curved needles as well as needles with arbitrary shape. If the needle has a fixed curvature, the location of the two tracked points can be used to calculate the curvature. For needles with an arbitrary

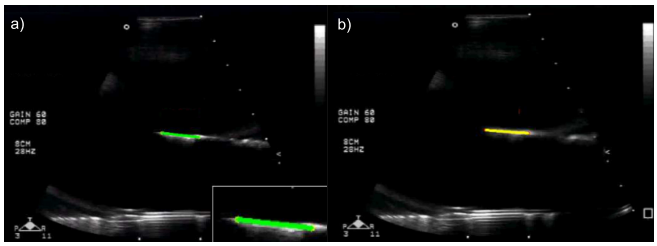

Fig. 8. a) Original pyramidal Lucas-Kanade optical flow algorithm, b) Pyramidal Lucas-Kanade optical flow algorithm with enhanced brightness. The detected angle is 5.8137° in the original pyramidal Lucas-Kanade optical flow algorithm and 4.0205° in the pyramidal Lucas-Kanade optical flow algorithm with enhanced brightness.

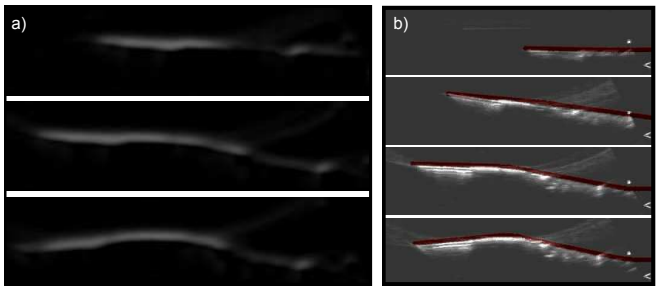

Fig. 9. a) After pre-processing and Sobel edge detection, the top surface of the cannula is clearly resolved, b) The algorithm is initialized when the cannula is straight and the kinematic model is overlayed on the ultrasound images as the cannula moves inside gelatin.

shape, multiple points can be selected such that a point cloud is formed on the top surface and the shape of the needle can be reconstructed from the point cloud.

IV. CONCLUSIONS

The accuracy of the image-guided needle-based procedures is highly dependent on the accurate detection of the needle position. This work presented an in-plane detection and an out-of-plane tracking algorithm for the discretely actuated steerable cannula. While detecting the needle tip, the ultrasound beam is generally assumed to be infinitely thin. Finite width of the ultrasound beam introduces tracking errors. Uniform cross-section of the needle tip aggravates the detection of the tip. The accuracy of the in-plane tracking is limited by the spatial resolution of the transducer. The method presented in this work provides a way to quantify the finite ultrasound beam width and the spatial accuracy of the ultrasound transducer. Hough circle transform was used to detect the cross-section of the cannula and it was demonstrated that the tip can be accurately detected. A brightness enhancement technique was developed to alleviate the brightness variation of the ultrasound images. This enabled using the pyramidal Lucas-Kanade algorithm to track the cannula configuration in-plane.

Our goal is to combine in-plane tracking and out-of-plane tracking to steer the discretely actuated steerable cannula in 3D. The methods and tools that are presented in this work form the foundation required to achieve this goal. In our previous work, we developed PWM (pulse width modulation)-based temperature feedback and PWM-based image feedback controllers to control the joint angles. Motion planning algorithms were also developed to generate a path between the entry point to the tissue and the target point. In our future work, we will combine these tools and do active ultrasound image-based tracking and control of the cannula to execute trajectories that are obtained using the motion planning algorithm.

REFERENCES

[1] E. Ayvali, C.P. Liang, M. Ho, Y. Chen, and J. P. Desai. Towards a discretely actuated steerable cannula for diagnostic and therapeutic procedures. *The International Journal of Robotics Research*, 31(5):588–603, 2012.

[2] G. Bradski. The opencv library. *Dr. Dobb's Journal of Software Tools*, 2000.

[3] S.P. DiMaio and S.E. Salcudean. Needle steering and model-based trajectory planning. In *Medical Image Computing and Computer-Assisted Intervention - MICCAI 2003*, volume 2878, pages 33–40, 2003.

[4] G. Fichtinger, J.P. Fiene, C.W. Kennedy, G. Kronreif, I. Iordachita, D.Y. Song, E. C. Burdette, and P. Kazanzides. Robotic assistance for ultrasound-guided prostate brachytherapy. *Medical Image Analysis*, 12(5):535 – 545, 2008.

[5] R. H. Gottlieb, W. B. Robinette, D. J. Rubens, D. F. Hartley, P. J. Fultz, and M. R. Violante. Coating agent permits improved visualization of biopsy needles during sonography. *American Journal of Roentgenology*, 171(6):1301–1302, 1998.

[6] C.L.L. Hendriks, M. van Ginkel, P.W. Verbeek, and L. J. van Vliet. The generalized radon transform: Sampling, accuracy and memory considerations. *Pattern Recognition*, 38(12):2494 – 2505, 2005.

[7] J. Hong1, T. Dohi1, M. Hashizume, K. Konishi, and N. Hata. An ultrasound-driven needle-insertion robot for percutaneous cholecystostomy. *Physics in Medicine AND Biology*, 49(3):441, 2000.

[8] J. Huang, J.K. Triedman, N.V. Vasilyev, Y. Suematsu, R.O. Cleveland, and Dupont P.E. Imaging artifacts of medical instruments in ultrasound-guided interventions. *J Ultrasound Med.*, 26(10):1303–22, 2007.

[9] B.D. Lucas and T. Kanade. An iterative image registration technique with an application to stereo vision. In *Proceedings of the international joint conference on Artificial intelligence,*, pages 674–679, 1981.

[10] V.G. Mallapragada, N. Sarkar, and T.K. Podder. Robot assisted real-time tumor manipulation for breast biopsy. In *IEEE International Conference on Robotics and Automation(ICRA)*, pages 2515–2520, 2008.

[11] H.R.S. Neshat and R.V. Patel. Real-time parametric curved needle segmentation in 3d ultrasound images. In *2nd IEEE RAS EMBS International Conference on Biomedical Robotics and Biomechatronics (BIOROB)*, pages 670–675, 2008.

[12] Z. Neubach and M. Shoham. Ultrasound-guided robot for flexible needle steering. *IEEE Transactions on Biomedical Engineering*, 57(4):799–805, 2010.

[13] P.M. Novotny, J. A. Stoll, N. V. Vasilyev, P. J. del Nido, P. E. Dupont, T. E. Zickler, and R. D. Howe. Gpu based real-time instrument tracking with three-dimensional ultrasound. *Medical Image Analysis*, 11(5):458 – 464, 2007.

[14] M Torabi, K. Hauser, R. Alterovitz, D. Vincent, and K. Goldberg. Guiding medical needles using single-point tissue manipulation. In *in Proceedings of the IEEE International Conference on Robotics and Automation*, pages 2705–2710, 2009.

[15] G.J. Vrooijink, M. Abayazid, and S. Misra. Real-time three-dimensional flexible needle tracking using two-dimensional ultrasound. In *Proceedings of the IEEE International Conference on Robotics and Automation (ICRA)*, 2013.